Electronic Supplementary Material (ESI) for Journal of Materials Chemistry A.

Supporting Information

Highly efficient construction of hollow Co-N_x nanocube cages dispersion implanting with porous carbonized nanofibers for Li-O_2 batteries

School of Energy and Environmental Engineering, University of Science and Technology Beijing, Beijing 100083, China; Beijing Key Laboratory of Resource-oriented Treatment of Industrial pollutants, Beijing 100083, China; Energy Conservation and Environmental Protection Engineering Research Center in Universities of Beijing, Beijing 100083, China.

Corresponding author: congjuli@126.com

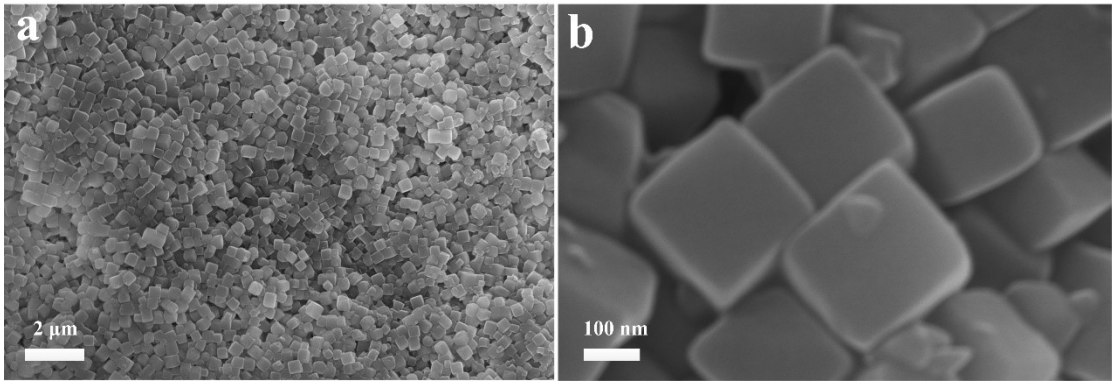

Fig. S1. SEM images of cubic ZIF-8 at different magnifications.

As the amount of the surfactant CTAB increases, the faster the crystal nucleation speed, the smaller the size of the cube ZIF-8.

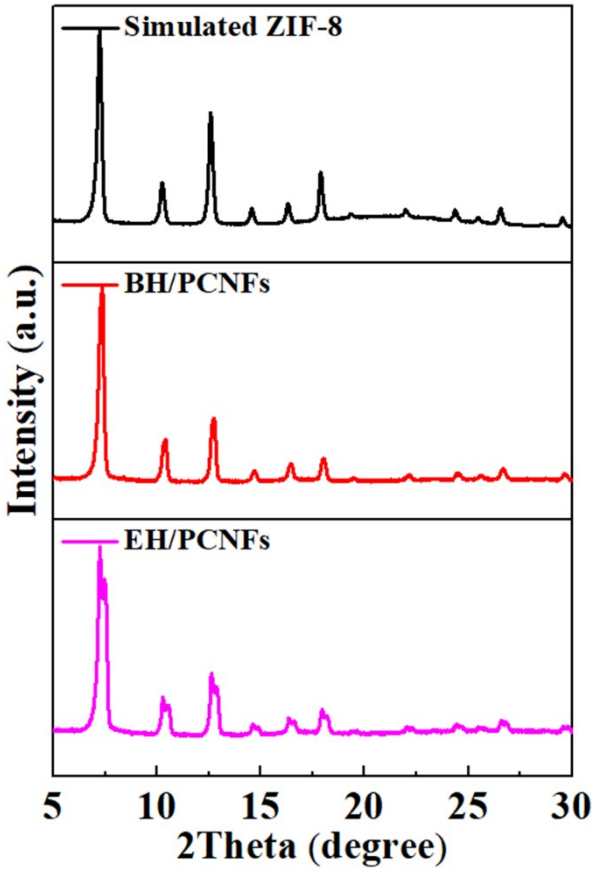

Fig. S2. XRD patterns of as-prepared of EH/PCNFs(a) and BH/PCNFs (b).

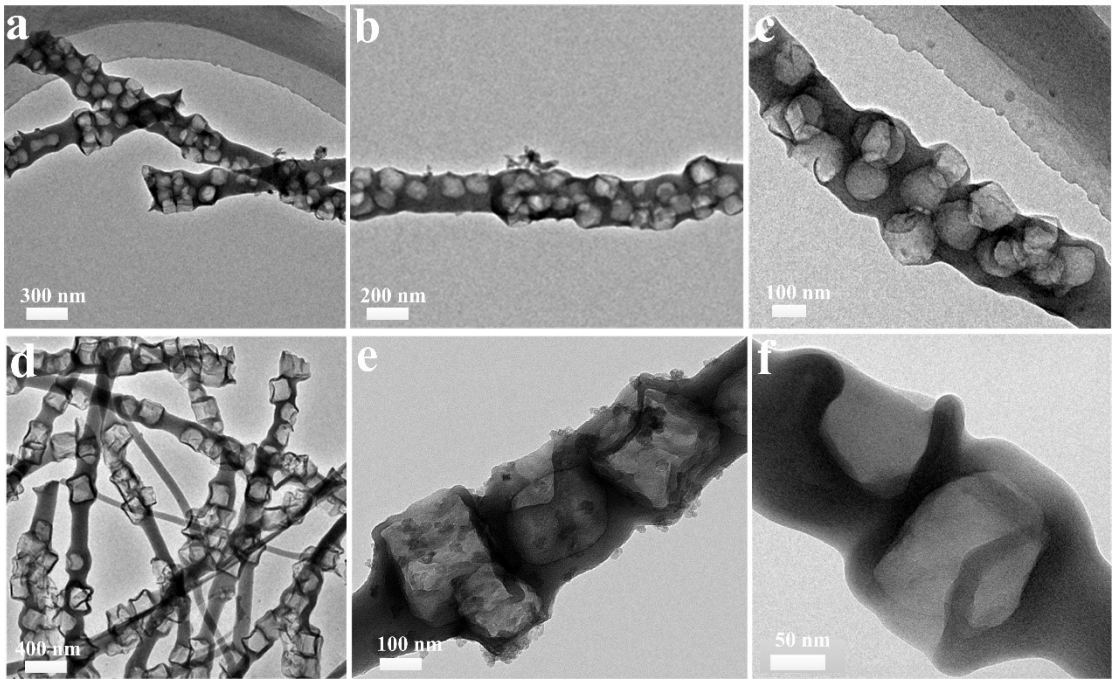

Fig. S3. FE-SEM images of EH/PCNFs(a-c) and BH/PCNFs(d-f) under different magnifications.

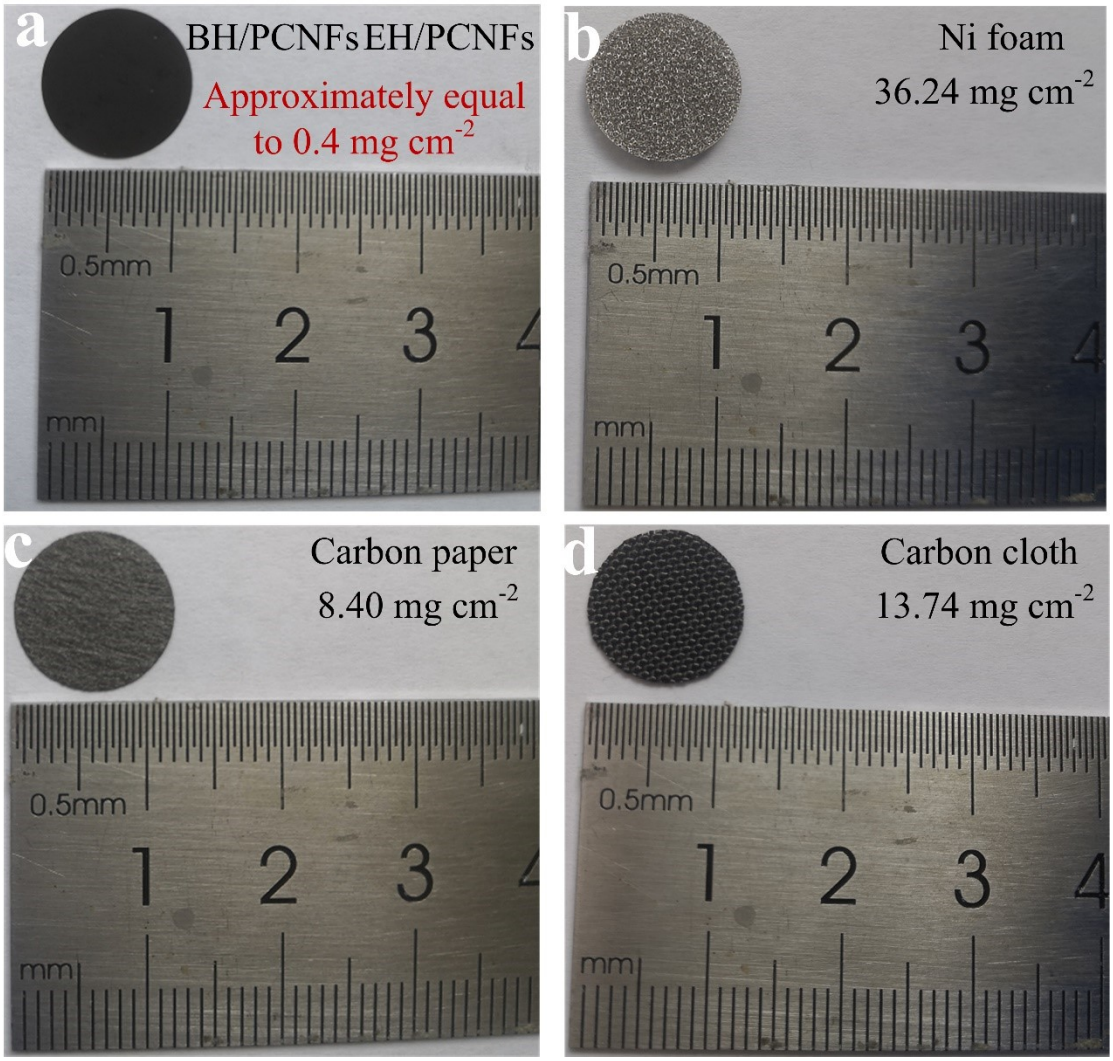

Fig. S4. The optical photographs of various electrodes with a diameter of 12 mm and their corresponding mass (a-d).

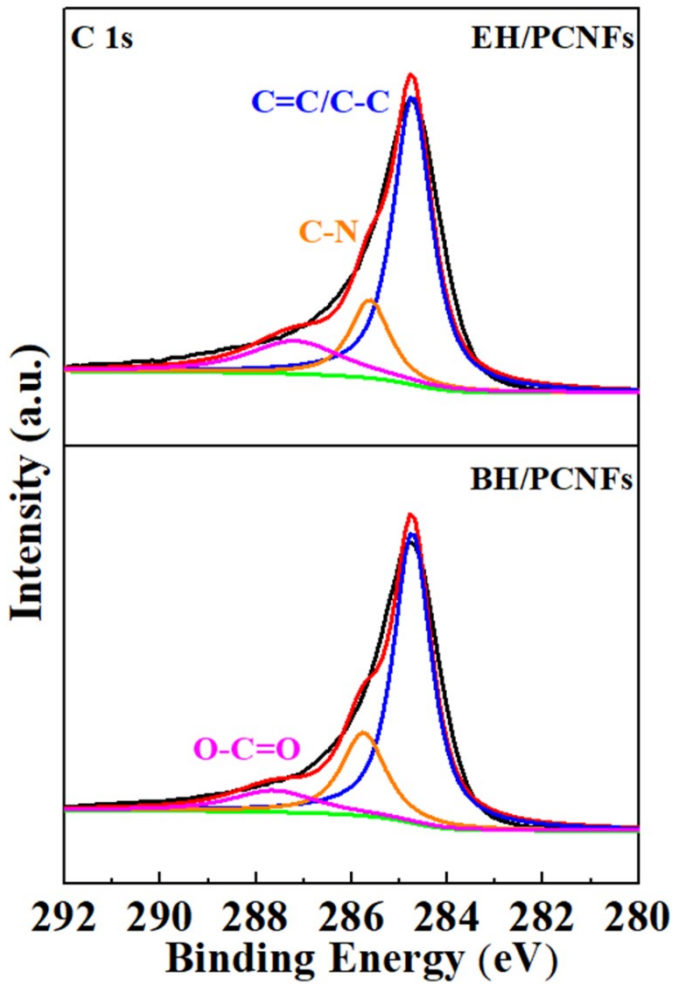

Fig. S5. The X-ray photoelectron spectroscopy (XPS) measurement of EH/PCNFs and BH/PCNFs.

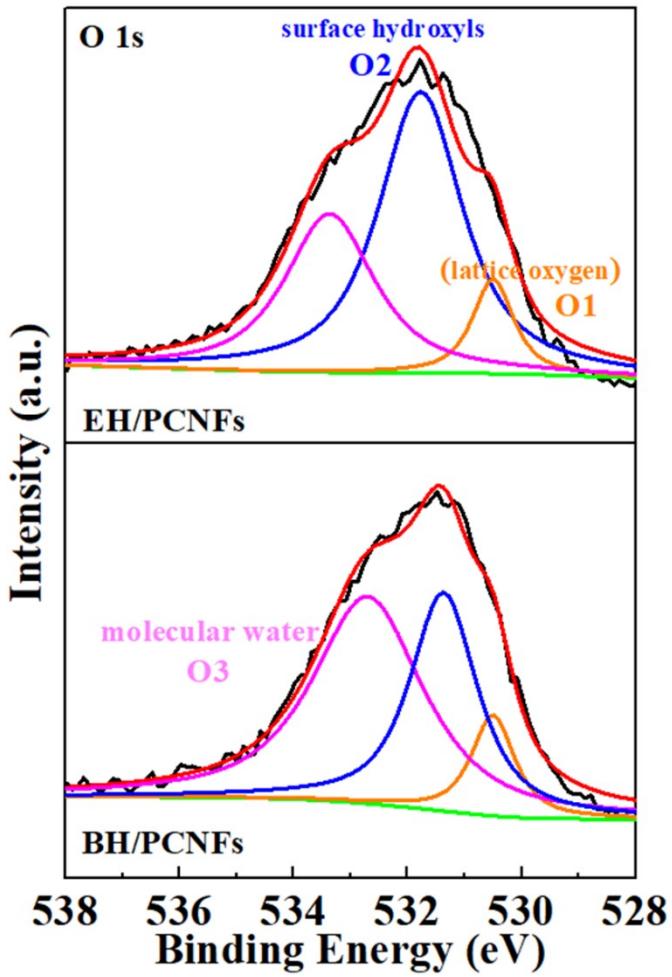

Fig. S6. The X-ray photoelectron spectroscopy (XPS) measurement EH/PCNFs and BH/PCNFs.

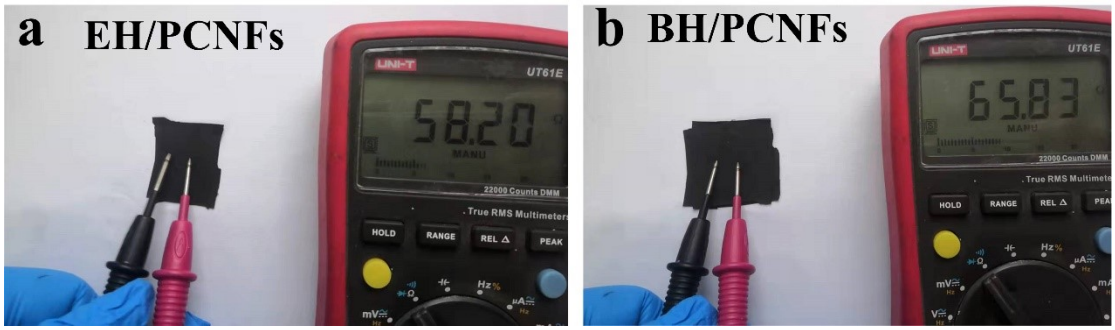

Fig. S7. the conductivity values of the prepared two electrodes. (a) EH/PCNFs; (b) BH/PCNFs.

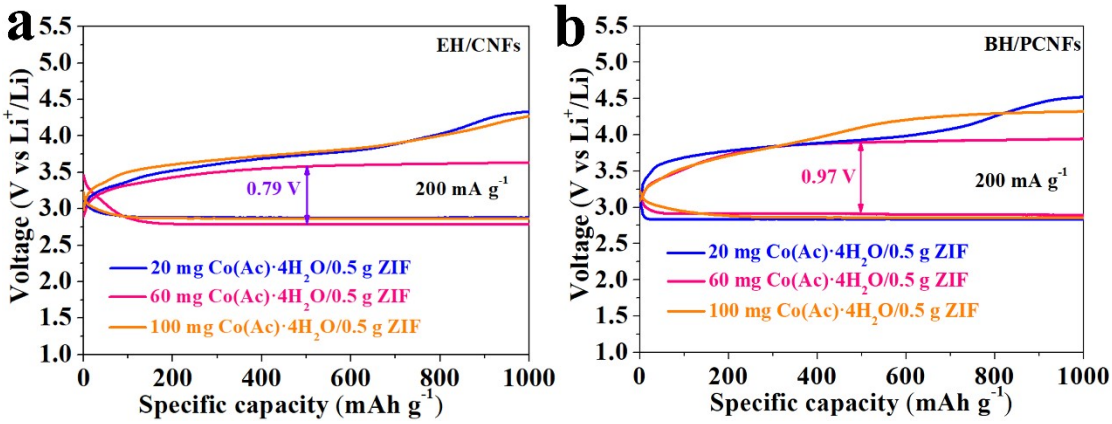

Fig. S8. The discharge-charge voltage curves of BH/PCNFs and EH/PCNFs electrodes under different electrospinning parameters with cut-off capacity of 1000 mAh g^{-1}.

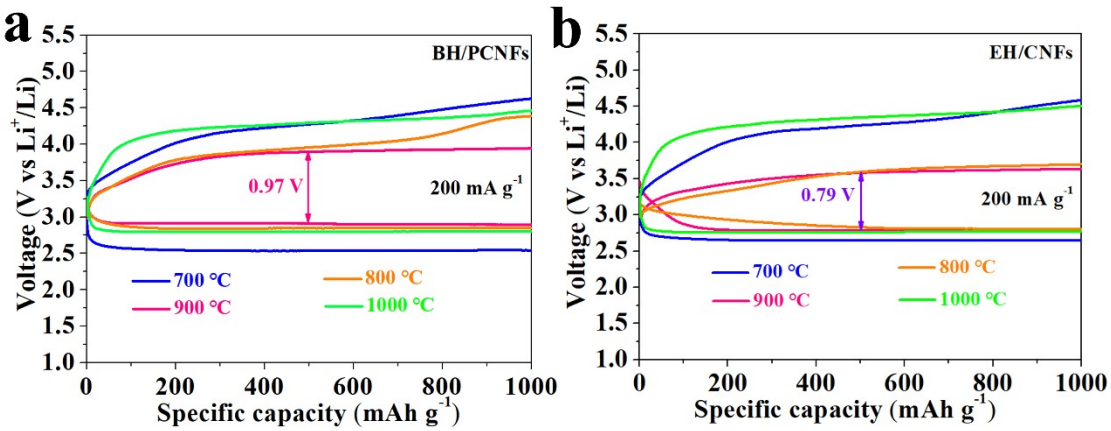

Fig. S9. The discharge-charge voltage curves of BH/PCNFs and EH/PCNFs electrodes under different annealing conditions with cut-off capacity of 1000 mAh g^{-1}.

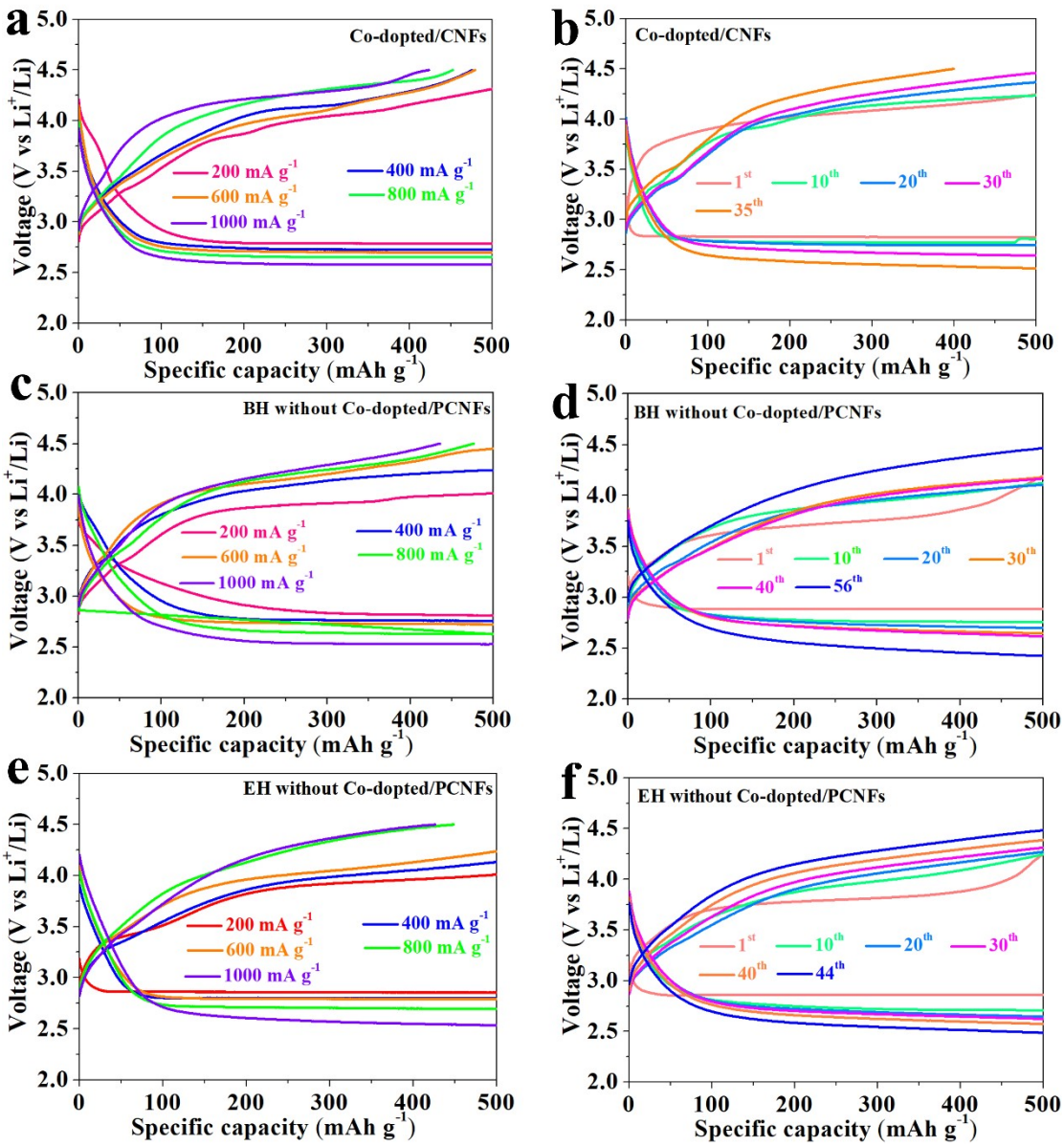

Fig. S10. The discharge-charge voltage curves of Co-dopted/CNFs, BH without Co-dopted/PCNFs and EH without Co-dopted/PCNFs electrodes under different current densities with cut-off capacity of 500 mAh g^{-1} (a, c, e);the long cycle curves of Co-dopted/CNFs, BH without Co-dopted/PCNFs and EH without Co-dopted/PCNFs electrodes under current density of 200 mA g^{-1} with cut-off capacity of 500 mAh g^{-1} (b, d, f).

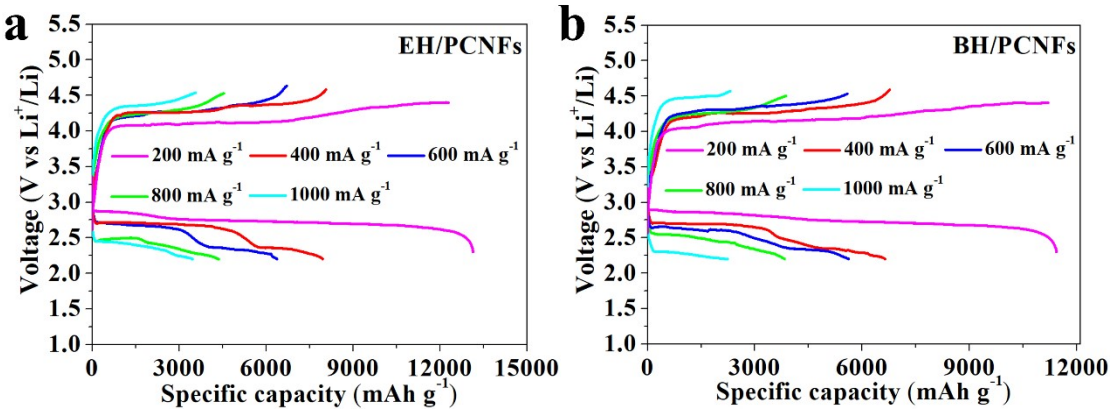

Fig. S11. (a, b) the initial deep discharge–charge profiles.

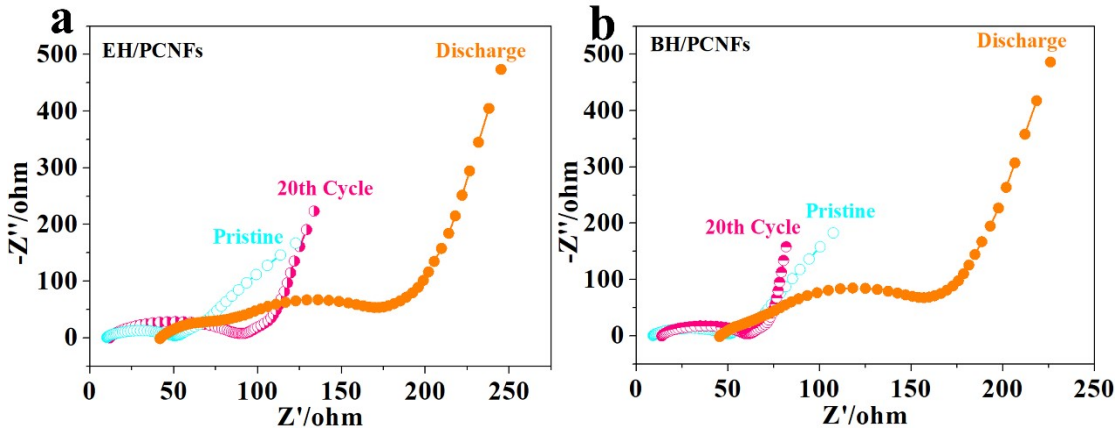

Fig. S12. Nyquist plots of LOBs with BH/PCNFs or EH/PCNFs electrode under different electrochemical states of original state, discharge to 500 mAh g^{-1}, and charge to 500 mAh g^{-1} (a-b).

Table S1. ICP-OES results of BH/CNFs and EH/CNFs catalysts.

Catalyst	Co (wt%)
EH/PCNFs	1.27
BH/PCNFs	1.32

Table S2. The information of BET surface area, total pore volume, pore width of as-prepared two samples.

Samples	S_{BET} (m^2/g)	V_{total} (cm^3/g)	V_{micro} (cm^3/g)	Pore width (nm)	Pore size (nm)
EH/PCNFs	128.92	0.13	0.12	4.10	~2, 100
BH/PCNFs	30.54	0.14	No detected	No detected	No detected

Table S3. Summary and comparison of LOBs performance with BH/CNFs and EH/CNFs-based electrocatalysts.

Catalysts	Maximum Capacity		Cycling performance			Ref.
	Capacity (mAh g^{-1})	Current (mA g^{-1})	Cycles	Current (mA g^{-1})	Capacity (mAh g^{-1})	
BH/PCNFs	**11442**	200	**143**	200	500	This work
EH/PCNFs	**13162**	200	**117**	200	500	This work
α- MnO_2/C	1400	100	43	100	500	[1]
$LaNiO_3$/4 h	5910	50	50	250	500	[2]
Pt/NiO	2329	100	47	100	800	[3]
Co_3O_4-H	5220	200	100	200	500	[4]
Ni-Fe LDHs-V_{Ni}	5823	100	88	100	500	[5]
p-CNT/Co_3O_4	5107	100	116	200	500	[6]
Co_3O_4/CNTs/CFP	7196.5	200	40	100	500	[7]
α- MnO_2@GN	2500	50	47	100	1000	[8]
Co-cage	12400	200	132	500	1000	[9]
Ag@LFO	8476	200	174	100	1000	[10]
Ag/g-C_3N_4/Co_3O_4	7723	100	51	500	1000	[11]
Porous Carbonized Co_3O_4 Inverse Opals	6959	100	29	100	1000	[12]
NiO/Ti_3C_2-2	13350	100	90	500	500	[13]
Co SAs@N-C	20105	200	260	400	1000	[14]

Reference

1 Y. Qin, J. Lu, P. Du, Z. Chen, Y. Ren, T. Wu, J. T. Miller, J. Wen, D. J. Miller, Z. Zhang and K. Amine, *Energy Environ. Sci.*, 2013, **6**, 519–531.

2 J. Zhang, C. Zhang, W. Li, Q. Guo, H. Gao, Y. You, Y. Li, Z. Cui, K. C. Jiang, H. Long, D. Zhang and S. Xin, *ACS Appl. Mater. Interfaces*, 2018, **10**, 5543–5550.

3 H. Dong, P. Tang, X. Wang, K. Li, Y. Wang, D. Wang, H. Liu, S. Yang and C. Wu, *ACS Appl. Mater. Interfaces*, 2019, **11**, 39789–39797.

4 Y. Zheng, R. Gao, L. Zheng, L. Sun, Z. Hu and X. Liu, *ACS Catal.*, 2019, **9**, 3773–3782.

5 Y. Zhou, D. Yan, Q. Gu, S. Zhu, L. Wang, H. Peng and Y. Zhao, *Appl. Catal. B Environ.*, 2020, **285**, 119792.

6 Y. Zhou, Z. Lyu, L. Wang, W. Dong, W. Dai, X. Cui, Z. Hao, M. Lai and W. Chen, *J. Mater. Chem. A*, 2017, *5*, 25501–25508.

7 Y. guo Huang, J. Chen, X. hui Zhang, Y. hui Zan, X. ming Wu, Z. qiang He, H. qiang Wang and Q. yu Li, *Chem. Eng. J.*, 2016, **296**, 28–34.

8 Y. Cao, M. Sen Zheng, S. Cai, X. Lin, C. Yang, W. Hu and Q. F. Dong, *J. Mater. Chem. A*, 2014, **2**, 18736–18741.

9 Z. Jiang, H. Sun, W. Shi, T. Zhou, J. Hu, J. Cheng, P. Hu and S. Sun, *Nano Res.*, 2019, **12**, 1555-1562.

10 Y. Cong, Q. Tang, X. Wang, M. Liu, J. Liu, Z. Geng, R. Cao, X. Zhang, W. Zhang, K. Huang and S. Feng, *ACS Catal.*, 2019, **9**, 11743–11752.

11 Q. Guo, C. Zhang, C. Zhang, S. Xin, P. Zhang, Q. Shi, D. Zhang and Y. You, *J. Energy Chem.*, 2020, **41**, 185–193.

12 S. A. Cho, Y. J. Jang, H. D. Lim, J. E. Lee, Y. H. Jang, T. T. H. Nguyen, F. M. Mota, D. P. Fenning, K. Kang, Y. Shao-Horn and D. H. Kim, *Adv. Energy Mater.*, 2017, **7**, 1700391.

13 X. Li, C. Wen, M. Yuan, Z. Sun, Y. Wei, L. Ma, H. Li and G. Sun, *J. Alloys Compd.*, 2020, **824**, 153803.

14 P. Wang, Y. Ren, R. Wang, P. Zhang, M. Ding, C. Li, D. Zhao, Z. Qian, Z. Zhang, L. Zhang and L. Yin, *Nat. Commun.*, 2020, **11**, 1576-1576.